

F. Alonso-Marroquín, R. García-Rojo & H. J. Herrmann

ICAI, University of Stuttgart,

Pfaffenwaldring 27, 70569 Stuttgart, Germany

The quasi-static mechanical response of granular materials under cyclic loading is studied in this paper using a discrete polydisperse model of disks. The response of the system is characterized by a linear accumulation of plastic deformation with the number of cycles. At the grain level, a quasi-periodic ratchet-like behavior is observed at the contacts. The study of this slow dynamics allows to explore the role of friction in the permanent deformation of unbound granular materials supporting streets and roads.

1 INTRODUCTION

Traditional pavement design methods are still almost completely empirical. Long term experience with the performance of on-service roads is supplemented with the results obtained from especially constructed test pavements. Changes in loading and environmental conditions can therefore be hardly considered or treated as parameters, limiting the scope of the information obtained. These disadvantages of the traditional methods have become more obvious during the last decades as a consequence of the grow of transportation needs. The increase of traffic loads have resulted in a rapid deterioration of the public road system and therefore in a rise of the maintenance expenses. This has attracted the attention of public authorities that is urging the road construction industry to optimize the designs. The use of recycled materials and by-products as alternatives to the natural aggregates used in pavement structures is also claimed nowadays. All these urges and needs have forced the development of new methods that can be more versatile and comprehensive.

Mechanistic and analytical design procedures have been developed based on the analysis of the response of the structure under specific loads and environmental conditions. Understanding the behavior of the components of the structure is of course a prerequisite of this approach. In this respect, elastoplastic behavior of unbound granular materials (basic component of roads and pavement) has been one of the main of pavement engineering for many years (1; 2), since they are principal responsible of the rutting and cracking of the pavement. Unbound granular materials exhibit two types of deformation when subjected

to cyclic loading: resilient deformation which could lead to fatigue cracking of the overlaying bound, and permanent deformation. Note that although the permanent deformation occurred in one cycle is only a small fraction of the overall deformation in the pavement, the gradual accumulation of these plastic deformations could lead to an eventual failure of the material due to excessive rutting. Whether a given system will experience progressive accumulation of permanent deformation, or whether the increase of permanent deformation will stop is crucial for the performance prediction. Most of the research carried out over the years concentrated on the resilient behavior, maybe due to the practical difficulties in studying permanent deformation. The use of simple models of the material permits the numerical resolution of the dynamics, which will be of great importance in the understanding of the granular components of pavements. In particular, a detailed study of the micro-mechanics of the permanent strain in the system is then possible.

The response of unbound soil under cyclic loading has been investigated introducing the *shakedown theory* (2; 3; 4). This theory predicts that a pavement is liable to show progressive accumulation of plastic strains under repeated loading if the magnitude of the applied loads exceeds a limiting value called the shakedown limit. The pavement is then said to exhibit an *incremental collapse*. On the other hand, if the loads are under this limit, the growth of plastic deformations will eventually level off and the pavement is said to have attained a state of shakedown by means of adaptation to the applied loads. More in detail, the shakedown concept maintains that there are four cat-

egories of material response under repeated loading:

- An *elastic* range for low enough loading levels, in which no permanent strains occurs.
- *elastic shakedown*, where the applied stress is slightly under the plastic shakedown limit. The material is plastic for a finite number cycles. However the ultimate response is elastic.
- *plastic shakedown*, where the applied stress is slightly less than that required to produce rapid incremental collapse. The material achieves a long-term steady state response with no accumulation of plastic strain and hysteresis.
- *Incremental collapse or ratcheting*, where the applied repeated stress is relatively large. Plastic strains accumulate rapidly with failure occurring in the relatively short term.

Shakedown theory is essentially an extension of the classical theory of elastoplasticity. This theory the cyclic loading response by postulating the existence of an elastic region in the stress space (5). This elastic region is a pragmatic compromise which helps to give a dependence of response on the recent history of the deformation, but is not a necessary feature. Element tests show indeed that the onset of the plastic deformation is gradual and not sharply defined. The bounding surface model have been proposed in order to provide a more appropriate description (6). This theory has not found widespread in the geotechnical application, due to its complex mathematical structure and the great number of parameters in it, that are difficult to calibrate (7).

Ten years ago, the hypoplastic model was formulated in order to mend the deficiencies of the elastoplastic theory (8; 9). The term *hypoplastic* refers to the fact that any load involves plastic deformations. Without any recourse to an elastic regime, the hypoplastic models established the incremental stress-strain relation with the Cauchy stress tensor and void-ratio as internal variables. Latter versions of the hypoplastic equations provide a correct description of the historical dependence of the mechanical response, introducing additional internal variables such as the back stress tensor (9) or the inter-granular strain (10). These model have been skeptically received by the engineering community, due to scarce physical meaning of these internal variables.

Most of the theoretical work trying to identify the internal variables of the constitutive equations are based on macro-mechanical observations of the response of soils samples in conventional apparatus. A micro-mechanical observation of the phenomena,

would help to get an insight into these internal variables. Indeed, the mechanical response of the granular soils is no more than a combined response of many micro-mechanical arrangements, such as inter-particle slips, breakage of grains and wearing of the contacts.

In the last years, grain scale investigation of cyclic loading behavior of granular materials has become possible using discrete element methods, in which the evolution of the individual grain is obtained by the calculation of the interaction between the particles. The quasi-static coulomb friction on lasting contacts has been extensively studied by means of algorithms of molecular dynamic (MD) (11) and contact dynamic (CD) (12). In the MD method an elastic regime is introduce in each contact, and the evolution of the grains is solved explicitly by the numerical solution of the motion equations. In the CD approach the particles are supposed infinitely hard, and the equilibrium equations are solved by using an implicit algorithm (13). The grain are usually represented by spheres or disks. More realistic geometries, that have already been used (14; 15), are limited by the high computational time that those simulations require.

Recent micro-mechanical investigation of granular materials point out the singular disorder of these media. Experiments and simulations show strong fluctuations in contact forces (16) and their long range correlation through chain forces. It will be shown in this paper that a ratcheting behavior can be found in a simple 2D disk model, as a direct consequence of this particular disorder of the contact network. A periodic irreversible motion at the sliding contacts is observed when a cyclic loading is applied. The existence of ratcheting motion in the sliding contact will be shown. These *ratchets* in the sliding contacts produce long time regimes with a constant rate of accumulation of permanent deformation.

The model used is described in Sec. 2, where the inter-particle interactions are also detailed. The dynamics of the system is solved by means of a MD algorithm. The evaluation of the stress-strain relation during cyclic loading and the accumulation of permanent deformation is presented in Sec. 3. A grain scale investigation of the cyclic loading response is performed in Sec.4 by the evaluation of the distribution of the contact forces. The connection between the micro-mechanical observation and the macro-mechanical response is also discussed. Finally, the concluding remarks and future perspectives of this work are presented in Sec. 5

2 MODEL

MD algorithms have been used to simulate granular materials via polygonal particles (17; 18; 19). A scheme will be considered in this paper, being the

grains modeled by disks. With this further idealization, we try to identify the influence of the geometry of the grains on some interesting responses of the system (19; 15). Being the algorithm faster for spheres than for polygons, we expect to reach longer ranges of the cyclic loading process. A suitable contact force must be introduced in order to include the quasi-static frictional force and the sliding condition.

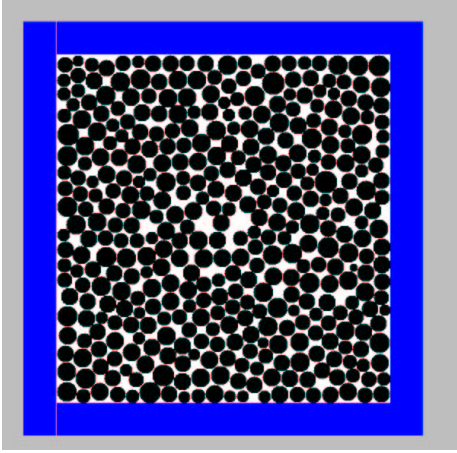


Figure 1: Packing of the disks. The system is closed by four walls that are initially subjected to a certain fixed pressure. The cyclic loading is imposed through the walls at the top and the bottom, while the other two walls push with a steady stress.

Disks, representing the particles, are so generated that the diversity of their areas follows a Gaussian distribution with mean value ℓ^2 and variance of $0.36\ell^2$.

2.1 Contact forces.

In order to calculate the forces, we assume that all the disks have a characteristic thickness L . The force between two disks is written as $\vec{F} = \vec{f}L$ and the mass of the disks is $M \cdot L$. In any real contact, there is deformation in the impact region. In the calculation of the contact, the disks are supposed to be rigid, but they are allowed to overlap so that the force can be calculated by means of this virtual overlap.

The contact force can be broken down in $\vec{f}^c = \vec{f}^e + \vec{f}^v$, where \vec{f}^e and \vec{f}^v are the elastic and viscous contribution. The elastic part of the contact force also splits in two components, $\vec{f}^e = f_n^e \hat{n}^c + f_t^e \hat{t}^c$. Where $\hat{n}^c = (\vec{r}_i - \vec{r}_j) / |\vec{r}_i - \vec{r}_j|$ and \hat{t}^c is perpendicular to \hat{n}^c . It is worth it to discuss these components carefully.

2.1.1 Normal elastic forces.

The normal elastic force is defined $f_n^e = -k_n \delta$, where k_n is the normal stiffness and δ is the overlapping length. Given two particles i and j with diameter d_i and d_j , respectively, their overlapping length is defined as

$$\delta = \frac{1}{2}(d_i + d_j) - (\vec{r}_i - \vec{r}_j) \cdot \vec{n}, \quad (1)$$

in terms of the position vector \vec{r}_i of particle i and the unit vector \vec{n}^c that points from i to j .

2.1.2 Friction forces.

In order to model the quasi-static friction force, the elastic tangential force is calculated using an extension of the method proposed by Cundall-Strack (14): An elastic force $f_t^e = k_t \Delta x_t$ proportional to the elastic displacement is included at each contact. k_t is the tangential stiffness. The elastic displacement Δx_t is calculated as the time integral of the tangential velocity of the contact during the time that the elastic condition $|f_t| < \mu f_n$ is satisfied. Here μ is the friction coefficient. The sliding condition is imposed keeping this force constant when $|f_t| = \mu f_n$. The straightforward calculation of this elastic displacement is given by the time integral starting at the beginning of the contact

$$\Delta x_t^e = \int_0^t v_t^c(t') \Theta(\mu f_n^e - |f_t^e|) dt', \quad (2)$$

where Θ is the Heaviside step function and \vec{v}_t^c denotes the tangential component of the relative velocity \vec{v}^c at the contact. \vec{v}^c depends on the linear velocity \vec{v}_i and angular velocity $\vec{\omega}_i$ of the particles in contact according to

$$\vec{v}^c = \vec{v}_i - \vec{v}_j - \vec{\omega}_i \times \frac{d_1}{2} \vec{n}^c + \vec{\omega}_j \times \frac{d_2}{2} \vec{n}^c. \quad (3)$$

2.1.3 Damping forces.

A rapid relaxation during the preparation of the sample and a reduction of the acoustic waves produced during the loading is obtained if damping forces are included. These forces are calculated as $\vec{f}^v = m\nu\vec{v}^c$. Here m is the relative mass of the disks in contact and ν is the coefficient of viscosity. These forces introduce time dependence effects during the cyclic loading. Nevertheless, it will be shown in Sect 4 that these effect can be arbitrarily reduced by increasing the time of loading, so that we can assume the quasi-static approximation to be valid.

2.2 Sample preparation.

The way in which the sample is prepared for the experiment, has a strong influence on the mechanical response of the granular material. In our case, the disks are first placed randomly into a rectangular box such that they do not overlap with each other. The interaction of the disks with the walls of the box is implemented applying a normal visco-elastic force $f_n^w = -k_n \delta - m\nu_n v_n^c$ at each disk lodged in any of the walls. Here δ is the penetration length of the disk on the wall. A gravitational field $\vec{g} = g\vec{r}$ is also switched

on, where \vec{r} is the vector connecting the center of mass of the assembly with the center of the disk. The activation of this gravity field produces homogeneous, isotropic distribution of disks.

After a certain time t_0 , (which is defined below) a change in the gravity modulus is imposed such as $g = g_0 + 1/2(g_f - g_0)(1 + \cos(100\pi t/t_0))$ until the time $2t_0$ in order to bring the porosity down. Samples with packing fraction around 0.819 ± 0.001 are obtained after relaxation with this method if $g_f = 100g_0$ (g_0 will be defined next).

The external load is imposed by applying a force $\sigma_1 W$ and $\sigma_y H$ on the horizontal and vertical walls, respectively. W and H are correspondingly the width and the height of the sample. When the velocity of the disks vanishes, the gravity is switched off. A fifth-order predictor-corrector algorithm is used to solve the equations of motion.

It can be shown by dimensional analysis that the strain response depends only on a minimum set of dimensionless parameters: 1) the ratio t_0/t_s , between the period of cyclic loading t_0 and the characteristic period of oscillation $t_s = \sqrt{k_n/\rho\ell^2}$ (where k_n is the normal stiffness of the contacts and ρ the density of the grains). 2) The ratio t_r/t_s between the relaxation time $t_r = 1/\nu$ and the oscillation time. 3) the ratio k_t/k_n between the stiffnesses. 4) the adimensional stress state σ/k_n and 5) the friction coefficient $\mu = 0.1$. In our simulation we take $t_0 = 1000t_s$, $t_r = 100t_s$, $k_t = 0.33k_n$, $g_0 = 6.25 \times 10^{-8}k_n$, and the initial pressure $p_0 = 6 \times 10^{-4}k_n$. Finally, $t_s = 2.5 \times 10^{-5}s$ and $k_n = 160MPa$.

3 PERMANENT DEFORMATION

In the simulation of the cyclic loading response we use a procedure equivalent to the element laboratory biaxial test. Initially, the sample is isotropically compressed until the pressure p_0 is reached. Then, the stress $\sigma_y = p_0$ is kept constant, while the vertical one is changed in time $\sigma_x = p_0 + \frac{\sqrt{2}}{4}\Delta\sigma[1 + \cos(\pi t/t_0)]$.

3.1 Stress-strain calculation.

In terms of the strain components $\epsilon_x = \frac{\Delta W}{W}$ and $\epsilon_y = \frac{\Delta H}{H}$, the shear strain $\gamma = \epsilon_x - \epsilon_y$ has been obtained in the simulations. The volume fraction is also calculated as $\Phi = V_p/V_b$, where V_p is the sum of the areas of the disks, and V_b the total volume of the system.

Part (a) of Figure 2 shows the relation between the shear stress $q = (\sigma_x - \sigma_y)/2$ and the shear strain γ in the case of a loading amplitude $\Delta\sigma = 0.2p_0$. This relation consists of open hysteresis loops which narrows as consecutive load-unload cycles are applied. This process produces an accumulation of permanent strain with the number of cycles which is represented by γ_N in part (c) of Figure 2. We observe that the

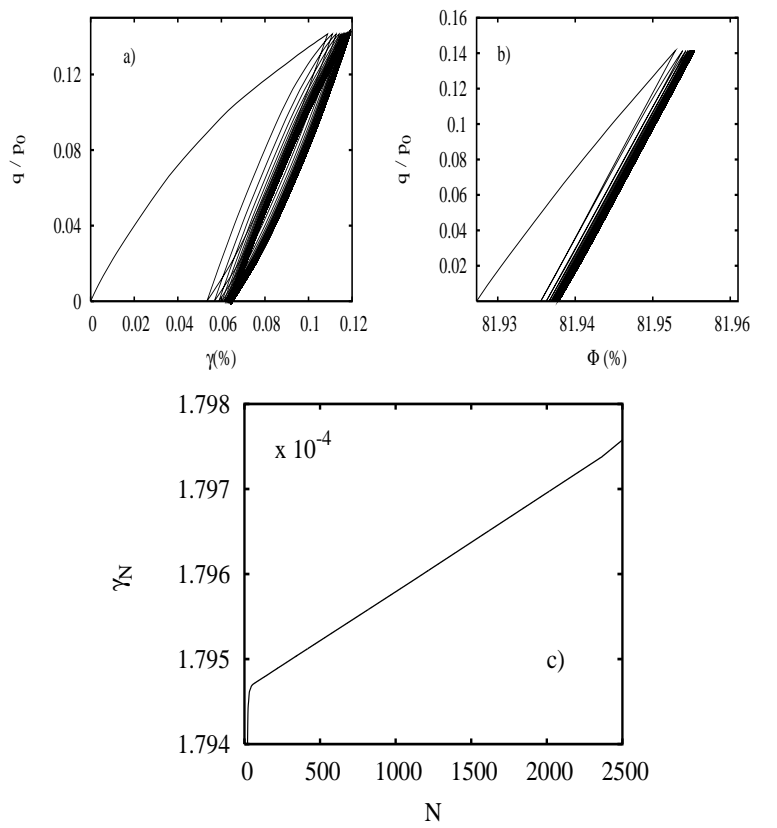


Figure 2: (a)Up left: Shear stress versus shear strain in the first 40 cycles. (b) Up right: permanent (plastic) strain γ_N after N cycles versus the number of cycles. (c)Bottom: stress against the volume fraction in the longer range.

strain response consists of a short time regime, with rapid accumulation of plastic strain, and a *ratcheting* regime, with a constant accumulation rate of plastic strain of around 2.3×10^{-9} per cycle. In longer simulation a sequence of different ratcheting regimes, separated by short plastic deformations, can be observed (15).

Part (b) of Figure 2 shows the relation between the shear stress and the volume fraction. This consists of asymmetric compaction-dilation cycles which makes the sample to compact during the cyclic loading. We observe a slow variation of the fraction during the *ratcheting* regime. The evolution of the volume ratio seems to be rather sensitive to the initial random structure of the disks. Even so, we found that after 1.8×10^3 cycles the volume fraction still slowly increasing linearly the sample, without any evidence of a saturation level.

3.2 Applicability of the shakedown theory.

It might be expected that for amplitudes of the loading cycles small enough, the elastic regime postulated in the shakedown theory could be reached (7). In an attempt to detect the existence of this elastic regime, we decreased the amplitude of the load cycles and evaluated the corresponding asymptotic response. In

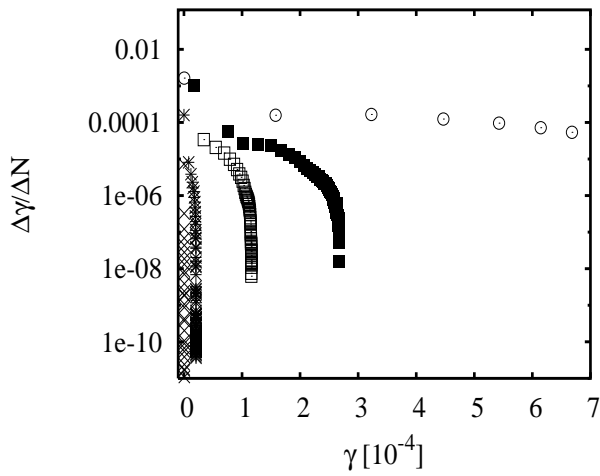


Figure 3: Cumulative permanent strain versus permanent strain rate. Crosses correspond to $\Delta\sigma = 0.01$, stars $\Delta\sigma = 0.1$, boxes $\Delta\sigma = 0.2$, solid boxes $\Delta\sigma = 0.3$ and circles $\Delta\sigma = 0.4$.

Figure 3, the change of the strain rate with the cumulative strain is plotted. Coincidentally with the experimental results in (4), we found a transition from a plastic shakedown regime to an incremental collapse. The plastic shakedown occurs for very low stresses: the system first reacts to the loading with a transient plastic deformation, becoming resilient after that. If very high stress are applied the system shows an incremental plastic deformation with each loading cycle. This behavior in a pavement would result in its failure by shear deformation. Between these regimes, the system shows an intermediate response. In this intermediate region, the plastic shakedown shown in Figure 3 turns to a linear growth of the strain for longer time. This latter behavior can be clearly observed in part (c) of 2, but was not included in Figure 3.

3.3 Quasi-static limit.

Concerning to role of the inertial effect in this ratcheting regime, the same test has been applied on five identical samples, imposing different loading frequencies in each one of test. The result, shown in Figure 4, is that as the frequency is reduced, the ratcheting effect gets progressively smaller until a quasi-static regime is reached. In this regime a reduction of one half of the frequency does not affect the strain response in more of 5%. From Figure 4, it can be concluded that damping or inertial effects do not affect the apparition of ratcheting in the sample.

4 MICRO-MECHANICAL INVESTIGATION

The existence of these ratcheting regimes with constant accumulation of plastic deformation per cycle suggests a certain periodic behavior in the sliding contacts. This behavior is apparently in contradiction with the strong temporal fluctuations that has been observed in granular materials (20). We have noticed,

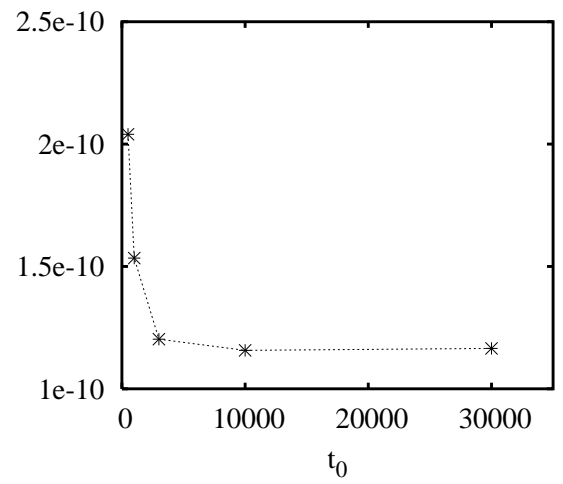


Figure 4: Variation of the plastic deformation per cycle with the duration of the cyclic loading t_0 .

however, a the persistence of the probability distribution of forces trough the cyclic loading that can explain this particular behavior.

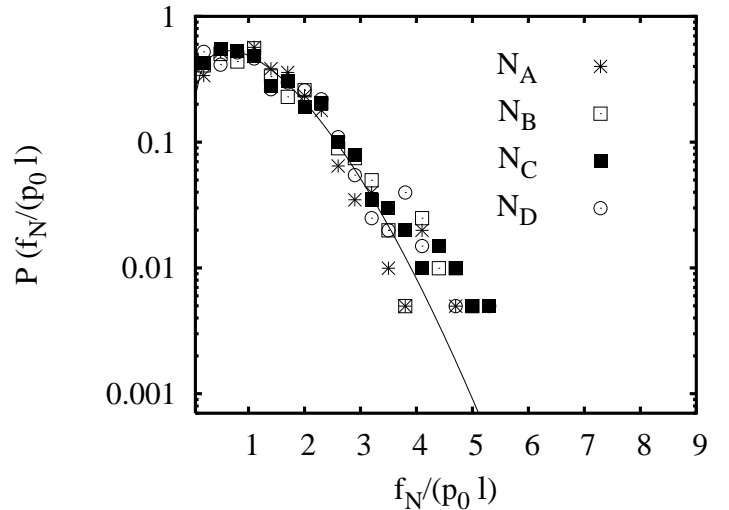


Figure 5: Distribution function of the normal forces in the contacts, measured in four different times of the simulation: $N_A = 10$, $N_B = 105$, $N_C = 150$ and $N_D = 190$. Note that the mean radius ℓ used in the scaling of the force, has been previously defined. In this simulation $\Delta\sigma = 0.1$. The equation of the best fit curve is: $0.843x^{0.431} \exp -0.546x^{1.630}$.

4.1 Fluctuations on the force.

Despite the uniformity of the granular materials, the distribution of forces within the materials seems to be very heterogeneous. The stress applied on the boundary is transmitted through chains where the contact forces are particularly strong (16). In Figure 5 the distribution function of normal forces at four different snapshots of the simulation is shown. The best-fit curve is also included for an easier comparison. Note that although all distributions were measured in different times of the simulation, they correspond to the

same stage of the cyclic loading. It is clearly observed that the shape of the distribution of forces at this point remains approximately constant throughout the whole simulation. This has also been checked following the time evolution of the first and the second moment of the distribution.

4.2 Field of displacements.

Figure 6 shows a snapshot of one of our simulations. The displacements of the particles previous to the snapshot are shown in arbitrary units. Two opposite flows of particles can be observed as a consequence of the cyclic stress. These particular shearing of the particles is responsible of the observed strain growth in the direction. Interesting is to note also the formation a vortex structure. This phenomenon rise the question of which the relation strain/structure-formation is. This a matter however that escapes the scope of this paper.

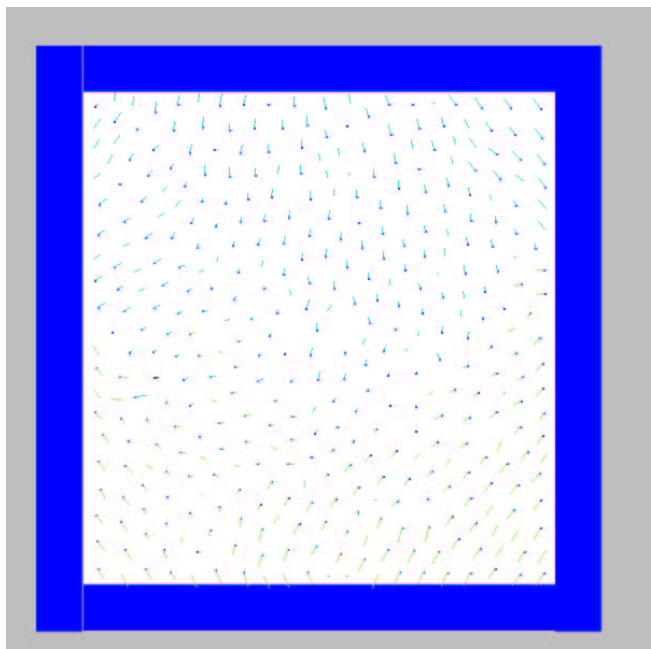


Figure 6: Snapshot of the simulation of a system with $\Delta\sigma = 0.1$. This image correspond to the instant $N=130$, in which the system is already in a ratcheting regime. The lines represent the previous displacement of the particles.

4.3 Sliding contacts.

One of the most important features of the force network is the high number of sliding contacts. Although most of the contacts satisfy the elastic condition $|f_t| < \mu f_n$, the strong heterogeneities of the force network produce a considerable amount of contacts reaching the sliding condition $|f_t| = \mu f_n$ during the compression. Those sliding contacts carry most of the irreversible deformation of the granular assembly during the cyclic loading. Opening and closure of contacts

are quite rare events, and the coordination number of the packing keeps approximately its initial value in all the simulations.

Let us next discuss the correlation between the dynamics of the sliding contacts and the evolution of the stiffness of the material. The last one is given by the slope of the stress strain curve in part (a) of Figure 2. The evolution of the fraction $n_s = N_s/N_c$ of sliding contacts with the number of loading cycles is shown in Figure 7. Here N_s is the number of sliding contacts and N_c is the total number of contacts. each loading phase, the number of sliding contacts increases, giving rise to a continuous decrease of the stiffness as shown in part (a) of Figure 2. An abrupt reduction of the number of sliding contacts is observed at the transition load-to-unload, producing a discontinuity in the stiffness and hence, a plastic deformation. Some contacts reach this almost periodical sliding state even for extremely small loading cycles. The ratchet-like behavior of these contacts produces a net displacement of the hysteretic stress-strain loop in each cycle, ruling out an elastic regime.

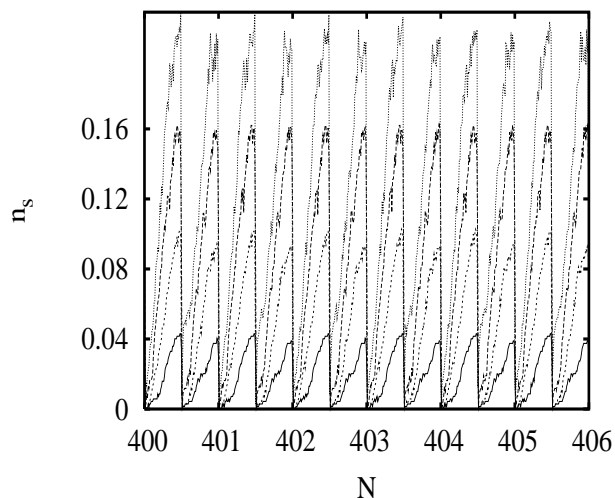


Figure 7: Ratio of sliding contacts n_s in the ratcheting for different values of $\Delta\sigma/p_0$: 0.1 (solid line), 0.2 (dotted line), 0.3 (dashed line), 0.4 (dotted top line).

5 CONCLUDING REMARKS

A grain scale investigation of the cyclic loading response of a packing of disks has been presented. We have shown the existence of long time regimes with a constant accumulation of plastic deformation per cycle, due to ratcheting motion at the sliding contacts. This phenomenon may have deep implications in the study of the permanent deformation of soils subjected to cyclic loading. More precisely, it may be necessary to introduce internal variables in the constitutive relations, connecting the dynamics of the sliding contacts with the evolution of the continuous variables during cyclic loading.

The coincidence of results with the elastoplastic behavior reported in polygonal packing, indicates that these phenomena do not depend on the geometry of the grains, and that they are inherent to the granular interactions. It is still open the question of the existence of ratcheting in three dimensional systems. Contact Dynamics seems to be the most appropriate method for the simulation of these systems, since MD becomes very expensive from the computational point of view. If similar responses of the system were found via CD simulation, it could be also confirmed that ratcheting in these systems is not a consequence of the MD method for the resolution of the dynamics of the system.

6 ACKNOWLEDGMENTS

The authors want to acknowledge the EU project *Degradation and Instabilities of Geomaterials with Application to Hazard Mitigation* (DIGA) in the framework of the Human Potential Program, Research Training Networks (HPRN-CT-2002-00220)

REFERENCES

- [1] F. Lekarp, A. Dawson, and U. Isacsson, *J. Transp. Engrg.* **126**, 76 (2000).
- [2] R. W. Sharp and J. R. Booker, *Journal of Transportation Engineering* **110**, 1 (1984).
- [3] F. Lekarp and A. Dawson, *Construction and Building Materials* **12**, 9 (1998).
- [4] S. Werkmeister, A. R. Dawson, and F. Wellner, *Jnl. Transportation Research Board* **1757**, 75 (2001).
- [5] D. Drucker and W. Prager, *Q. Appl. Math.* **10**, 157 (1952).
- [6] Y. F. Dafalias, *J. of Engng. Mech* **112**, 966 (1986).
- [7] *Constitutive Relations of soils*, edited by G. Gudehus, F. Darve, and I. Vardoulakis (Balkema, Rotterdam, 1984).
- [8] R. Chambon, J. Desrues, W. Hammad, and R. Charlier, *Int. J. Anal. Meth. Geomech.* **18**, 253 (1994).
- [9] D. Kolymbas, I. Herle, and P. A. Wolfferdorff, *Int. J. Anal. Meth. Geomech.* **19**, 415 (1995).
- [10] A. Niemunis and I. Herle, *Int. J. Mech. Cohesive-Frictional Mater.* **2**, 279 (1996).
- [11] P. A. Cundall and O. D. L. Strack, *Géotechnique* **29**, 47 (1979).
- [12] M. Jean and J. J. Moreau, in *Proceedings of Contact Mechanics International Symposium* (Presses Polytechniques et Universitaires Romandes, Lausanne, Switzerland, 1992), pp. 31–48.

- [13] J. J. Moreau, in *Powders & Grains 93* (Balkema, Rotterdam, 1993), p. 227.
- [14] P. A. Cundall, *Ingenieur-Archiv* **59**, 148 (1989).
- [15] F. Alonso-Marroquin and H. Herrmann, cond-mat/0305043 (unpublished).
- [16] F. Radjai, M. Jean, J. J. Moreau, and S. Roux, *Phys. Rev. Lett.* **77**, 274 (1996).
- [17] H.-J. Tillemans and H. J. Herrmann, *Physica A* **217**, 261 (1995).
- [18] F. Kun and H. J. Herrmann, *Comput. Methods Appl. Mech. Engrg.* **138**, 3 (1996).
- [19] F. Alonso-Marroquin and H. Herrmann, *Phys. Rev. E* **66**, 021301 (2002), cond-mat/0203476.
- [20] F. Radjai and S. Roux, *Phys. Rev. Lett.* **89**, 064302 (2002).